Experimental Investigation of Heat Transfer Characteristics on a Gas-to-Gas Parallel Flow Microchannel Heat Exchanger

Kohei Koyama* and Yutaka Asako

Department of Mechanical Engineering, Tokyo Metropolitan University, 1-1, Minami-Osawa, Hachioji, Tokyo, 192-0397, Japan

Abstract: Heat transfer characteristics of a gas-to-gas parallel flow microchannel heat exchanger have been experimentally investigated. Temperatures and pressures at inlets and outlets of the heat exchanger are measured to obtain heat transfer rates and pressure drops. The heat transfer and pressure drop characteristics are discussed. The results show that experimental pressure drop is approximately ten times as large as theoretically estimated pressure drop. Geometric configuration of the heat exchanger dominates pressure drop characteristics. The conventional log-mean temperature difference method and the constant wall temperature model proposed in our earlier work are applied to predict heat transfer rate of the parallel flow microchannel heat exchanger. Prediction accuracy of the log-mean temperature difference method is superior to that of the constant wall temperature model. Applicability of the log-mean temperature difference method depends on direction of fluid flow.

1. INTRODUCTION

Microscale devices have attracted many researchers in recent decades. Numerous literatures have been published on fluid flow and heat transfer characteristics of microchannels since Tuckerman and Pease [1] have demonstrated a heat sink with microchannels. Microchannel heat exchanger is a practical application of microscale channels. Developments of the heat exchanger yield miniaturization in engineering fields since it has a large area density, heat transfer area per unit volume. Several investigations have been conducted on a microchannel heat exchanger with liquid flow.

Bier *et al.* [2] have manufactured a crossflow microchannel heat exchanger by precision cutting. They tested the heat exchanger with water as a working fluid. A volumetric heat transfer coefficient of 324 MW m^{-3} K^{-1} was obtained. Friedrich *et al.* [3] have fabricated a micro crossflow heat exchanger by diamond machining. Trapezoidal-shaped channels were cut on a copper substrate. They tested with water, and their heat exchanger provided a volumetric heat transfer coefficient of nearly 45 MW m^{-3} K^{-1}. Ravigururajan *et al.* [4] have investigated on single-phase characteristics of a parallel microchannel heat exchanger. They used Refrigerant-124 as an experimental fluid. They showed that increase in heat transfer coefficient may be attributed to the thinking of the boundary layer in a narrow channel. Jiang *et al.* [5] have investigated on fluid flow and heat transfer performances of a microchannel heat exchanger and a micro-porous heat exchanger. Their results showed that heat transfer performance of the micro heat exchanger using porous media was better than that of the micro heat exchanger using microchannels, while the pressure drop of the former was much larger. They concluded that a microchannel heat exchanger with deep channels has the best overall thermal-hydraulic performance. Harris *et al.* [6] have fabricated and tested for both a polymer and a nickel micro crossflow heat exchanger. They summarized features of micro heat exchangers by comparing with those of high performance conventional scale automobile radiators. Alm *et al.* [7] have manufactured ceramic counterflow and crossflow microchannel heat exchangers. The experimental results were compared with estimated ones by standard heat exchanger correlations and numerical simulations using a porous body approach. They found that the geometry of the fluid channels was influenced by the joining process of the ceramic components.

Moreover, several researchers have used gaseous flow as a working fluid of a microchannel heat exchanger. Bier *et al.* [8] have tested on micro heat exchangers. Nitrogen, helium, and argon gases were used as a working fluid. They attained overall heat transfer coefficient up to 1700 W m^{-2} K^{-1} on a stainless steel heat exchanger by using helium. To estimate overall heat transfer coefficient, they proposed a homogeneous model used in a packed bed. The estimated results agreed well with experimental ones. Stief *et al.* [9] have conducted numerical simulations to determine the order of magnitude of optimal thermal conductivity of a micro heat exchanger. They found that heat transfer efficiency is a function of the heat conductivity of a wall, when nitrogen is used as the flow medium. They concluded that there exists an optimal thermal conductivity of a wall material. Miwa *et al.* [10] have conducted numerical computations on parallel and counterflow microchannel heat exchangers with gaseous flow. They discussed effects of compressibility of gaseous flow.

Authors have investigated heat transfer characteristics of a gas-to-gas counterflow microchannel heat exchanger [11]. In the earlier work, authors revealed that the conventional log-mean temperature difference method could not be employed for estimation of the heat transfer in the gas-to-gas counterflow microchannel heat exchanger. Then other heat

*Address correspondence to this author at the Department of Mechanical Engineering, Tokyo Metropolitan University, 1-1, Minami-Osawa, Hachioji, Tokyo, 192-0397, Japan; Tel: +81 42 677 2711; Fax: +81 42 677 2701; E-mail: koyama-kohei@ed.tmu.ac.jp
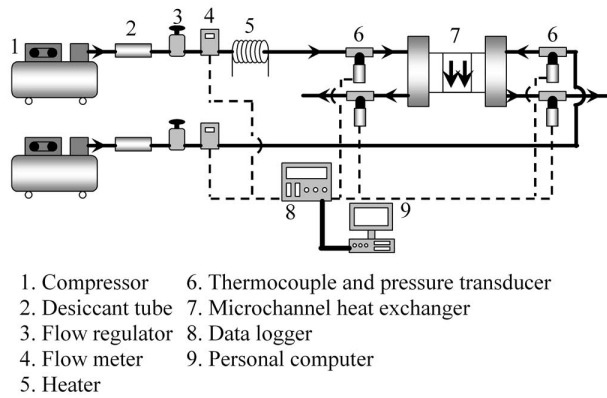
1. Compressor
2. Desiccant tube
3. Flow regulator
4. Flow meter
5. Heater
6. Thermocouple and pressure transducer
7. Microchannel heat exchanger
8. Data logger
9. Personal computer

Fig. (1). Schematic view of experimental setup.

exchange model with an assumption of constant partition wall temperature was proposed to predict heat transfer rate of the heat exchanger. Now authors focus on a parallel flow microchannel heat exchanger. Since a parallel flow microchannel heat exchanger has similar structure to a counterflow configuration, the conventional log-mean temperature difference method may not be employed. Investigation on heat exchange model of a parallel flow microchannel heat exchanger is required. The present study reports heat exchange model for a parallel flow microchannel heat exchanger.
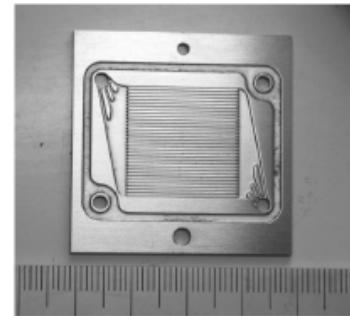
2. EXPERIMENTAL

2.1. Experimental Setup

Fig. (**1**) shows the schematic view of an experimental setup. It consists of two independent piping systems. One is for hot flow and the other is for cold flow. A piping system involves a compressor (1), a desiccant tube (2), a flow regulator (3), and a flow meter (4). The piping system of the hot flow includes a heater to heat working fluid. Air is used as the working fluid.

Airflow passes through the desiccant tube, the flow regulator, the flow meter, and flows into the microchannel heat exchanger, and is discharged to surroundings. The discharged air does not affect ambient conditions because a test room is large enough. Ambient air is compressed to be supplied as the working fluid by the compressor. The desiccant tube dehumidifies the airflow. The flow regulator (Kofloc, 2412L) controls a flow rate of the airflow and the flow meter (Kofloc, 3105-30SLM, accuracy: ±1.0 % F.S.) measures the flow rates. The heater heats the airflow on the hot passage. Temperatures at the inlets and the outlets of the heat exchanger are measured by T-type thermocouples. Pressures are simultaneously measured by the pressure transducers (Valcom, VESX500, max: 500 kPa, linearity: less than 0.25 %). The data logger (Eto Denki, CADAC21) acquires all data.

The microchannel heat exchanger is set in a box filled with spherical polystyrene foams, whose diameter is approximately 2 mm, to avoid heat leak from the heat exchanger to surroundings. Since polystyrene foam has a low thermal conductivity, it is suitable for an insulator. Note that the new polystyrene foams are used for each experiment because temperature of those is increased after an experiment.

The microchannel heat exchanger COMH manufactured by IMM (Institute für Mikrotechnik Mainz, Germany) is used for the experiments. The microchannels were fabricated by wet chemical etching on a stainless steel plate with length x width x thickness = 40 x 40 x 0.5 mm. This plate is used as a heat transfer plate. The microchannel has a rectangular cross section at 200 μm height and 300 μm width. This results in a hydraulic diameter of 240 μm. The channel length is 20 mm. A heat transfer plate contains 34 microchannels. Twenty plates are stacked and bolted to form the heat exchanger. Ten plates are used to the hot and cold passages of the heat exchanger, and which are stacked alternately. A heat transfer area of the heat exchanger is 6.8×10^{-3} m^2. Fig. **2** (**a**) shows a picture of the heat transfer plate and Fig. **2** (**b**) shows the microchannel heat exchanger COMH.

(a) Heat transfer plate.
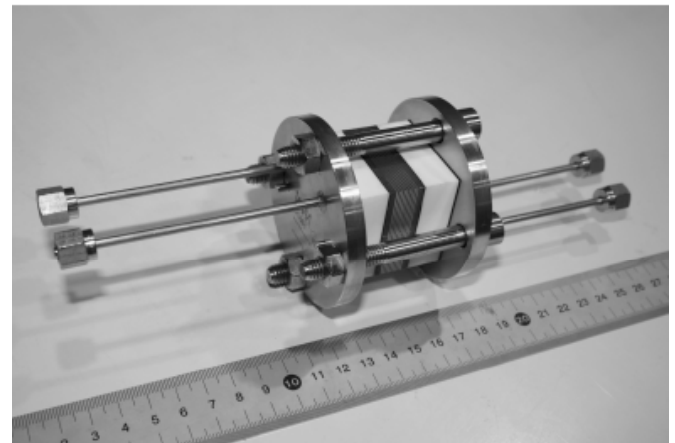
(b) Photograph of COMH.

Fig. (2). Microchannel heat exchanger COMH. (**a**) Heat transfer plate. (**b**) Photograph of COMH.

2.2. Experimental Procedure

Experiments are conducted under various flow rate conditions to investigate pressure drop and heat transfer characteristics of the microchannel heat exchanger. Volumetric flow rate under the standard state (0 °C, 1 atm) in both passages ranges from 5 to 15 L min^{-1}, the corresponding Rey-

nolds number ranges from 63.5 to 191. The flow should be laminar on whole experiments. Reynolds number Re is defined by

$$Re = \frac{\rho V D_h}{\mu} = \frac{2\dot{m}_{ch}}{\mu(a+b)} \tag{1}$$

where $\dot{m}_{ch}$ denotes a mass flow rate per channel, μ denotes a viscosity of air, and a and b denote a channel height and width, respectively.

The gage pressure at outlet of the compressors is maintained at 0.3 MPa. The airflow temperature of the hot passage at the inlet of the heat exchanger is maintained at approximately 75 °C, while the airflow of the cold passage is supplied from the compressor at a room temperature. The inlet temperature of the cold passage ranges from 14.2 to 20.3 °C.

Airflow is supplied by opening a valve of the compressor. Volumetric flow rates are controlled by using the flow regulators within ±0.5 % of arbitrary flow rate. The airflow is simultaneously heated on the hot passage. The airflow temperature is maintained by controlling a voltage of the heater. Data are logged every second during five minutes after steady state is ensured. Steady state is assumed to be achieved when the variations of the outlet temperatures are within ±0.1 °C in 10 minutes. Results are discussed by averaged data throughout this study.

2.3. Experimental uncertainties

Uncertainty analyses have been carried out for data reduction. Uncertainty for a pressure drop is 0.31 %. The accuracy of the flow meter is ±1.0 % of full scale. Therefore, uncertainty for a mass flow rate is from 6.0 % to 2.0 %; corresponding volumetric flow rate is from 5 L min^{-1} to 15 L min^{-1}. Uncertainty for a heat transfer rate is from 6.1 % to 2.4 %.

3. RESULTS AND DISCUSSION

3.1. Pressure Drop

This section describes pressure drop characteristics of the microchannel heat exchanger. A pressure drop is measured by the pressure transducers which are equipped in upstream and downstream section of the heat exchanger. The heat exchanger and pressure measurement points are connected by a circular connection tube of which inner diameter is 1.78 mm. The pressure measurement points are 17 cm away from inlets or outlets of the heat exchanger. Therefore pressure drop in the connection tube is calculated to reduct them from the measured pressure drops.

Reynolds number in the connection tube ranges from 3860 to 11570; corresponding volumetric flow rate is from 5 L min^{-1} to 15 L min^{-1}. This means that the airflow in the tube is turbulent. Let the smooth tube be assumed, a friction factor f and a pressure drop Δp are as follows

$$f = 0.3164 Re^{-0.25} \tag{2}$$

$$\Delta p = f \frac{l}{d} \frac{\rho V^2}{2} \tag{3}$$

where l is connection tube length, d is connection tube diameter, ρ is air density, and V is mean airflow velocity in the connection tube. Fig. (**3**) plots experimental pressure drop of the hot passage of the heat exchanger Δp as a function of Reynolds number of the hot passage Re_h. The experimental pressure drops are designated by solid symbols. The open symbols will be indicated in the next section. The experimental pressure drops increase linearly as Reynolds number increases. The experimental pressure drops of the hot passage are almost same value regardless of Reynolds numbers of the cold passage.
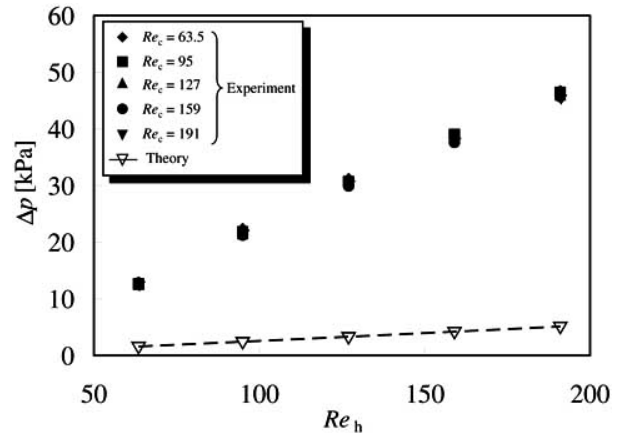

Fig. (3). Pressure drop characteristics.

3.2. Prediction of Pressure Drop

This section describes process to predict the pressure drop of the microchannel heat exchanger. The fluid passing through the heat exchanger is assumed as a continuum. This assumption is justified by Knudsen number Kn, which is defined by the ratio of mean free path λ and characteristic diameter D_h, as follows:

$$Kn = \frac{\lambda}{D_h} \tag{4}$$

In this study, Kn is 2.8×10^{-4}. This assures that the fluid is continuum.

Conventional theory on a duct flow is used to predict a pressure drop of the microchannel heat exchanger. For simplicity, airflow in the microchannels is assumed to be hydrodynamically fully developed. To predict a pressure drop, a friction factor f is required. Laminar flow friction factor of a rectangular duct is compiled by Shah and London [12]. In present study Poiseuille number $f \cdot Re$ is 14.7. The pressure drop in the channel is obtained by Eq. (5).

$$\Delta P = f \frac{\rho V^2 L}{2 D_h} \tag{5}$$

Effect of entrance pressure drop and exit pressure rise in the core of the heat exchanger should be considered because the area passing through the working fluid changes significantly. Kays and London [13] have summarized entrance and exit pressure drop as follows:

$$\frac{\Delta p_1}{\rho} = \frac{V^2}{2}(1-\sigma^2) + K_c \frac{V^2}{2} \tag{6}$$

$$\frac{\Delta p_2}{\rho} = \frac{V^2}{2}\left(1-\sigma^2\right) - K_e \frac{V^2}{2} \tag{7}$$

where Δp_1 and Δp_2 denote entrance pressure drop and exit pressure rise, respectively. σ, K_c, and K_e denote the ratio of core free-flow and frontal area ($\sigma = 0.34$), entrance pressure loss coefficients ($K_c = 1.14$), and exit pressure loss coefficients ($K_e = 0.18$), respectively. V denotes mean airflow velocity in a microchannel. Theoretical pressure drop Δp_{th} is given by

$$\Delta p_{th} = \Delta p_1 + \Delta p_{core} - \Delta p_2 \tag{8}$$

Fig. (**3**) compares Δp_{exp} and Δp_{th} as a function of Reynolds number of the cold passage Re_c. Δp_{exp} is approximately ten times as large as Δp_{th}. This is attributed to following factors.

(1) Pressure drop at Pressure Port

A T-shaped connector is used to connect the pressure transducer. The cross section of the passage in the connector is not uniform. There exists the pressure drop at the exit of the connector.

(2) Pressure Drop at Manifold Junction

Fig. (**4**) shows a schematic of the airflow manifold passage in the heat exchanger. Airflow is supplied to the heat exchanger manifold. Then the airflow divides into ten heat transfer plates at supply manifold junction. The airflow which passed through the microchannels combines at exhaust manifold junction. Flow dividing and combining cause additional pressure drop.
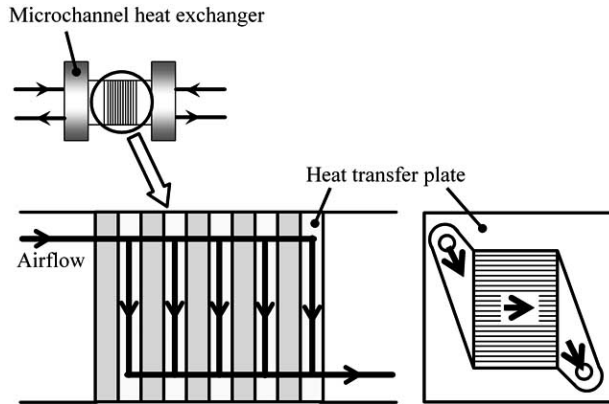

Fig. (4). Schematic view of the airflow.

(3) Nonuniformity of Flow Rate in Microchannels

The process described above assumes implicitly that the airflow is evenly supplied to all the heat transfer plates. However, the airflow divides unevenly to each heat transfer plate. Yin *et al.* [14] found that geometric configuration affects mass flow distribution of a microchannel heat exchanger. As shown in Fig. (**4**), the heat transfer plates are stacked in parallel. The diameter of the connection tube is 1.78 mm. Mean flow velocity attains 100 m s^{-1} when flow rate is 15 L min^{-1}. Since airflow divides at supply manifold junctions, pressure is significantly increased at downstream

supply manifold junction. On the other hand, pressure in the exhaust manifold decreases along flow direction. Consequently flow rate of the downstream plate will be the largest. Nonuniformity of flow rate in the microchannels increases pressure drop of the heat exchanger.

If these pressure losses are excluded from the total measured pressure drop, the pressure drop may be equal to the theoretical one. However, determination of the individual pressure loss is difficult due to measurement difficulty.

Effect of compressibility may affect pressure drop characteristics because air is compressible fluid. However, maximum Mach number of airflow in channels was 0.035. This means that effect of compressibility did not affect the experimental results.

3.3. Heat Transfer Rate

This section describes heat transfer characteristics of the microchannel heat exchanger. The first law of thermodynamics on the heat exchanger leads heat transfer rate expressed by Eqs. (9) and (10)

$$Q_h = \dot{m}_h c_p \left(T_{h,in} - T_{h,out}\right) \tag{9}$$

$$Q_c = \dot{m}_c c_p \left(T_{c,out} - T_{c,in}\right) \tag{10}$$

where c_p denotes specific heat at constant pressure and T denotes temperature. Subscripts h, c, in, and out stand for hot passage, cold passage, inlet, and outlet of the microchannel heat exchanger, respectively.

Although the microchannel heat exchanger is set in a box filled with spherical polystyrene foams for insulation, heat may leak to surroundings since the heat exchanger is not completely isolated. Fig. (**5**) shows the ratio of Q_c and Q_h as a function of Re_c. If the heat does not leak, Q_c / Q_h would be unity. However, values of Q_c / Q_h range from 0.92 to 1.25. The piping for hot and cold airflows lie in the insulating box in which the heat exchanger is set. Polystyrene foam beads are heated up and cooled down by heat from the piping. Then, temperature of the polystyrene beads takes the average temperature of hot and cold airflow, $T_m = (T_{h,in} + T_{c,in}) / 2$. When $\dot{m}_c \gg \dot{m}_h$, the temperature of the heat transfer plate becomes lower than T_m. Therefore the heat flows into the heat exchanger, namely $Q_c > Q_h$. When $\dot{m}_c \approx \dot{m}_h$, the heat transfer plate temperature becomes higher than T_m. Then
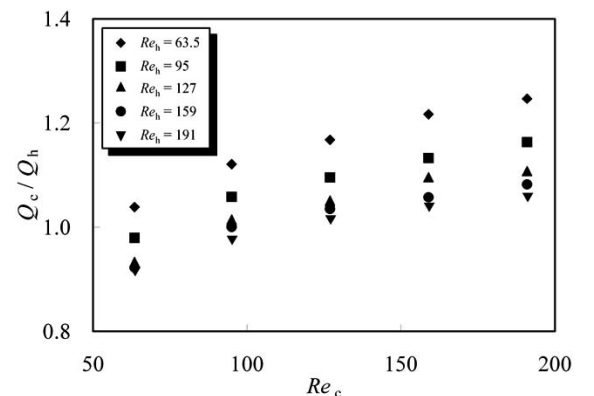

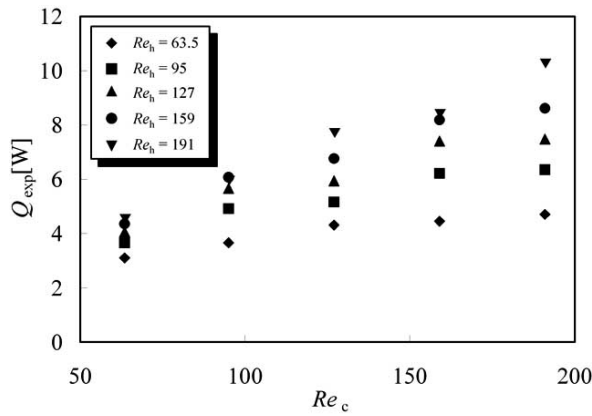**Fig. (5).** Relations between Re_c and Q_c / Q_h.

Fig. (6). Heat transfer rate of the parallel flow microchannel heat exchanger.

thermal balance will be $Q_h > Q_c$. When $\dot{m}_c \approx \dot{m}_h$, the heat transfer plate temperature is almost T_m. Then, $Q_h \approx Q_c$. Considering the fact, we have defined heat transfer rate Q_{exp} as follows:

$$Q = \frac{Q_h + Q_c}{2} \tag{11}$$

Fig. (**6**) plots the heat transfer rate as a function of Reynolds number in the cold passage Re_c, with the curve parameter of the Reynolds number in the hot passage Re_h. Heat transfer rate increases with increasing Re_c. A series of experiments has provided volumetric heat transfer rates up to 12.6 MW m^{-3}, the volumetric heat transfer rate represents heat transfer rate divided by total channel volume. Heat transfer rates for low Re_c take similar values, whereas they take different values depending on Re_h for large Re_c. Heat transfer rate may approach an asymptotic value by increasing Re_c. Unfortunately, experiments for large Reynolds number were not conducted due to a restriction of performance of the compressors.

Notice that qualitative tendencies of the heat transfer rates are similar to those of a conventional heat exchanger even though the working fluid is gas. A remarkable behavior on heat transfer has not been observed although gaeous fluid

flows in microscale channels. This is ascertained by Knudsen number which is extremely smaller than unity as described in section 3.2. Since the airflow can be regarded as continuum, the heat transfer characteristics exhibit a similar trend to those of conventional heat exchanger.

3.4. Prediction of Heat Transfer Rate

3.4.1. Log-mean Temperature Difference Method

Conventional log-mean temperature difference method is used to predict heat transfer rate of the heat exchanger. The correlation is expressed as

$$Q = AU\Delta T_{lm} \tag{12}$$

where A, U, and ΔT_{lm} denotes heat transfer area, overall heat transfer coefficient, and logarithmic mean temperature difference, respectively. ΔT_{lm} is defined by Eq. (13).

$$\Delta T_{lm} = \frac{\left(T_{h,in} - T_{c,out}\right) - \left(T_{h,out} - T_{c,in}\right)}{\ln\dfrac{T_{h,in} - T_{c,out}}{T_{h,out} - T_{c,in}}} \tag{13}$$

Calculation of a heat transfer rate in a channel requires Nusselt number Nu. Nusselt number in a channel depends on a thermal boundary condition of a channel wall. Shah and London [12] have summarized Nusselt number on rectangular ducts with fully developed flow. They obtained $Nu = 3.11$ for the constant wall temperature and the aspect ratio of 1.5. Although the thermal boundary condition of a channel wall cannot be preconditioned in the experiment, we use this value to calculate the overall heat transfer coefficient U which is defined as

$$\frac{1}{U} = \frac{1}{h_h} + \frac{t}{k} + \frac{1}{h_c} \tag{14}$$

Fig. (**7**) shows the heat transfer rate obtained by the experiment (EXP), Eq. (11), and the log-mean temperature difference method (LMTD), Eq. (12). The predicted heat transfer rate agrees well with the experimental results. The prediction error ranges from -4.2 % to -11 %. The conventional log-mean temperature difference method predicts heat transfer rate of the microchannel heat exchanger within an
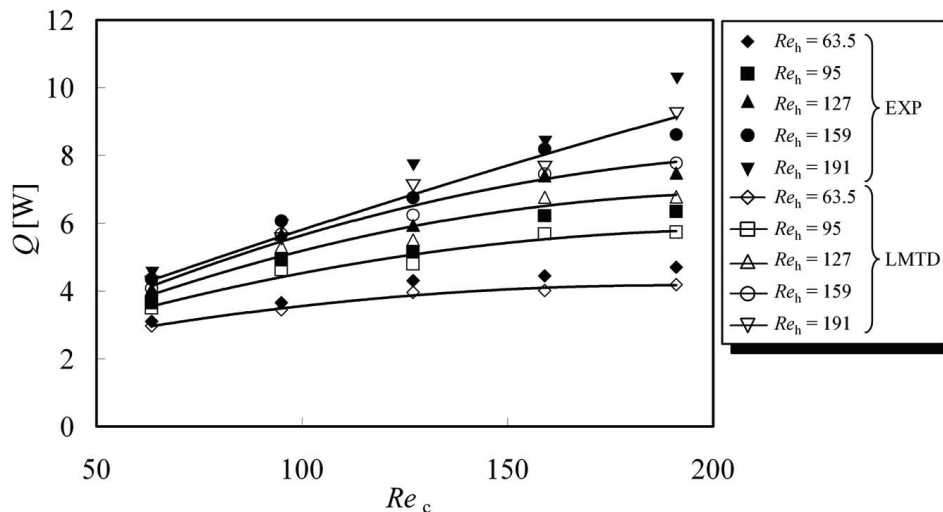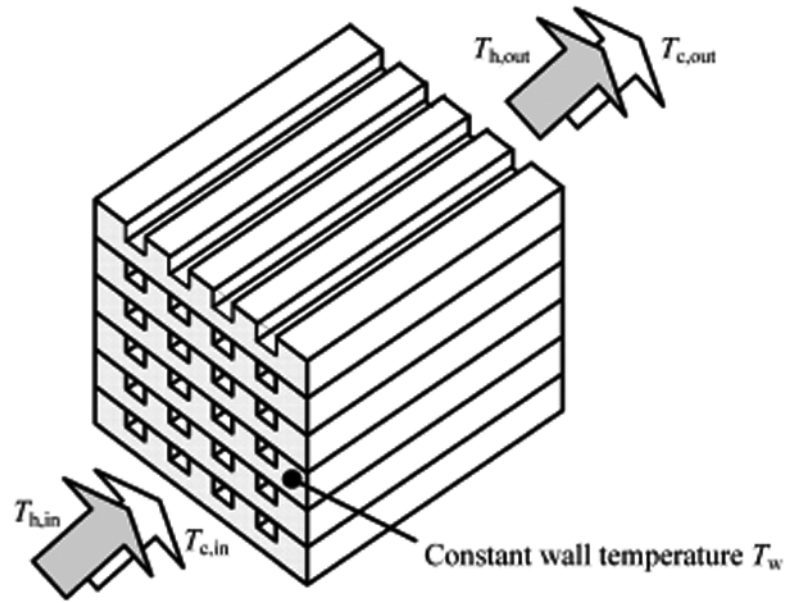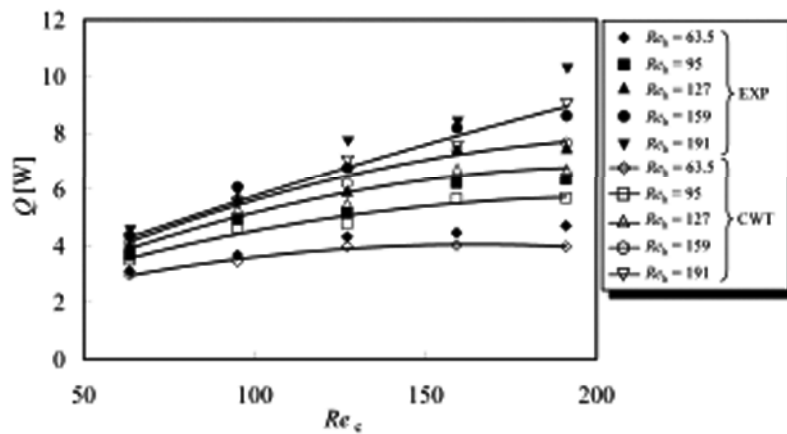

Fig. (7). Prediction of heat transfer rate using the log-mean temperature difference method.

(a)   Heat exchange model.

(b)   Prediction of heat transfer rate using the constant wall temperature model.

Fig. (8). Prediction of heat transfer rate. (**a**) Heat exchange model. (**b**) Prediction of heat transfer rate using the constant wall temperature model.

acceptable error.

3.4.2. Constant wall Temperature Model

In the earlier work [11], a heat exchange model which has a constant wall temperature was proposed to predict heat transfer rate of a gas-to-gas counterflow microchannel heat exchanger. The same model is applied to parallel flow heat exchanger in this section.

Fig. (**8**) (a) depicts a heat exchange model proposed. The configuration is the same as the heat exchanger tested.

Namely, a heat transfer plate has microchannels and the plates are stacked. Dimensions of the model are the same as those of the heat exchanger tested. Although a heat transfer plate of the heat exchanger tested contains 34 microchannels and 20 plates are stacked, four microchannels and six plates are drawn to avoid graphic complexity in Fig. **8** (**a**). Flow passing through the model is assumed to be steady, laminar, and fully developed flow. Inlet conditions such as temperatures and flow rates are the same as experimental ones. Considering the thermal energy balance of the model leads following correlations:

$$Q_{\text{h}} = Ah_{\text{h}} \frac{T_{\text{h,in}} - T_{\text{h,out}}}{\ln \dfrac{T_{\text{w}} - T_{\text{h,in}}}{T_{\text{w}} - T_{\text{h,out}}}} \tag{15}$$

$$Q_{\text{c}} = Ah_{\text{c}} \frac{T_{\text{c,out}} - T_{\text{c,in}}}{\ln \dfrac{T_{\text{w}} - T_{\text{c,in}}}{T_{\text{w}} - T_{\text{c,out}}}} \tag{16}$$

The microchannel has a rectangular cross section at 200 μm height and 300 μm width. This results in a hydraulic diameter of 240 μm. According to Shah and London [12], Nusselt number is 3.11 based on the hydraulic diameter with an assumption of constant wall temperature. The heat transfer coefficients h_{h}, and h_{c} in Eqs. (15) and (16) are obtained by $Nu = 3.11$. The heat transfer area A is 6.8×10^{-3} m^2. Note that thermal energy balance leads $Q = Q_{\text{h}} = Q_{\text{c}}$. There are five unknowns: $T_{\text{h,out}}$, $T_{\text{c,out}}$, T_{w}, Q_{h}, and Q_{c}. Combining Eqs. (9), (10), (15), (16), and $Q = Q_{\text{h}} = Q_{\text{c}}$, heat transfer rate can be obtained.

Fig. **8** (**b**) shows the heat transfer rate obtained by the experiment (EXP), Eq. (11), and the constant wall temperature model (CWT). The predicted heat transfer rate agrees well with the experimental results. The prediction error ranges from -4.2 % to -16 %. The constant wall temperature model predicts heat transfer rate well. However, the error is greater than that of log-mean temperature difference method described in section 3.4.1. The log-mean temperature difference method is superior to the constant wall temperature model on the parallel flow microchannel heat exchanger.

3.4.3. Applicability of the Log-Mean Temperature Difference Method

The conventional log-mean temperature difference method cannot be employed for the counterflow microchannel heat exchanger in earlier work [11]. In contrast, the method can be employed for the parallel flow microchannel heat exchanger in this study. Applicability of the log-mean temperature difference method is discussed in this section.

On a conventional-sized counterflow heat exchanger, maximum possible temperature change is difference of two inlet temperatures, $T_{\text{h,in}}$ - $T_{\text{c,in}}$. On a gas-to-gas counterflow microchannel heat exchanger, a large amount of heat is transferred in a partition wall since thermal conductivity of the wall is extremely larger than that of gas. Temperature of the partition wall T_{w} will be average temperature $T_{\text{m}} = (T_{\text{h,in}} + T_{\text{c,in}})$ / 2, namely $T_{\text{w}} \approx T_{\text{m}}$. Therefore $T_{\text{h,out}}$ does not drop below T_{w} and $T_{\text{c,out}}$ does not rise beyond T_{w}. Temperature behavior of a gas-to-gas counterflow microchannel heat exchanger differs from that of a conventional-sized counterflow heat exchanger. Consequently the conventional log-mean temperature difference method cannot be employed for a gas-to-gas counterflow microchannel heat exchanger.

Next attention will be turned to the parallel flow heat exchanger. On a microchannel parallel flow heat exchanger, outlet fluid temperatures in both passages will be equal to partition wall temperature T_{w} when heat is completely exchanged. Then the partition wall temperature will be average temperature, namely $T_{\text{w}} \approx T_{\text{m}}$. On a conventional-sized parallel flow heat exchanger, outlet temperatures in both passages will be T_{m} as well. Temperature behavior of a gas-to-gas

parallel flow microchannel heat exchanger is same as that of a conventional-sized parallel flow heat exchanger. Consequently the conventional log-mean temperature difference method can be employed for a gas-to-gas parallel flow microchannel heat exchanger. The fact means that applicability of log-mean temperature difference method depends on fluid flow direction.

4. CONCLUSION

Pressure drop and heat transfer characteristics of a gas-to-gas parallel flow microchannel heat exchanger have been experimentally investigated. We conclude that:

(1) Experimentally-obtained pressure drop is significantly larger than that obtained by conventional correlation. Geometric configuration of a heat exchanger dominates pressure drop characteristics.

(2) Conventional log-mean temperature difference method well predicts heat transfer rate of the parallel flow microchannel heat exchanger. The prediction error ranges from -4.2 % to -11 %.

(3) The prediction error of the constant wall temperature model ranges from -4.2 % to -16 %. The log-mean temperature difference method is slightly superior to the constant wall temperature model on the parallel flow microchannel heat exchanger.

(4) The conventional log-mean temperature difference method can be employed for a parallel flow heat exchanger regardless of heat exchanger size. Applicability of log-mean temperature difference method depends only on fluid flow direction.

NOMENCLATURE

A	=	heat transfer area, m^2
a	=	channel height, m
b	=	channel width, m
c_p	=	specific heat at constant pressure, J kg^{-1} K^{-1}
d	=	connection tube diameter, m
D_h	=	hydraulic diameter, m
f	=	friction factor
h	=	heat transfer coefficient, W m^{-2} K^{-1}
K_c	=	entrance pressure loss coefficient
K_e	=	exit pressure loss coefficient
Kn	=	Knudsen number, Eq. (2)
k	=	thermal conductivity, W m^{-1} K^{-1}
L	=	channel length, m
l	=	connection tube length, m
$\dot{m}$	=	mass flow rate, kg s^{-1}
Nu	=	Nusselt number

p	=	pressure, Pa
Q	=	heat transfer rate, W
Re	=	Reynolds number, Eq. (1)
T	=	temperature, K
U	=	overall heat transfer coefficient, W m^{-2} K^{-1}
V	=	velocity, m s^{-1}
λ	=	mean free path, m
μ	=	viscosity, Pa s
ρ	=	density, kg m^{-3}
σ	=	core free-flow/frontal area ratio

subscript

c	=	cold passage
ch	=	per channel
core	=	heat exchanger core
exp	=	experimental value
h	=	hot passage
in	=	inlet
out	=	outlet
th	=	theoretical value
w	=	wall

REFERENCES

[1]   D. B. Tuckerman, and R. F. W. Pease, "High-performance heat sinking for VLSI", *IEEE Electron Device Letter*, vol. EDL-2, No. 5, pp. 126-129, May 1981.

[2]   W. Bier, W. Keller, G. Linder, D. Seidel, and K. Schubert, "Manufacturing and testing of compact micro heat exchangers with high volumetric heat transfer coefficients", *ASME Dynamic Systems and Control Division (Publication) DSC*, vol. 19, pp. 189-197, 1990.

[3]   C. R. Friedrich, and S. D. Kang, "Micro heat exchangers fabricated by diamond machining", *Precision Engineering*, vol. 16, No. 1, pp. 56-59, January 1994.

[4]   T. S. Ravigururajan, J. Cuta, C. E. McDonald, and M. K. Drost, "Single-phase flow thermal performance characteristics of a parallel micro-channel heat exchanger", *ASME Heat Transfer Division, (Publication) HTD*, vol. 329, pp. 157-161, 1996.

[5]   P. X. Jiang, M. H. Fan, G. S. Si, and Z. P. Ren, "Thermal-hydraulic performance of small scale micro-channel and porous-media heat-exchanger", *Int. J. Heat Mass Transfer*, vol. 44, pp. 1039-1051, March 2001.

[6]   C. Harris, K. Kelly, T. Wang, A. McCandless, and S. Motakef, "Fabrication, modeling, and testing of micro-cross-flow heat exchangers", *J. Microelectromechanical Systems*, vol. 11, No. 6, pp. 726-735, December 2002.

[7]   B. Alm, U. Imke, R. Knitter, U. Schygulla, and S. Zimmermann ,"Testing and simulation of ceramic micro heat exchangers", *Chemical Engineering Journal*, vol. 135S, pp. S179-S184, January 2008.

[8]   W. Bier, W. Keller, G. Linder, D. Seidel, K. Schubert, and H. Martin, "Gas to gas heat transfer in micro heat exchangers", *Chemical Engineering and Processing*, vol. 32, pp. 33-43, February 1993.

[9]   T. Stief, O. U. Langer, and K. Schubert, "Numerical investigation of optimal heat conductivity in micro heat exchangers", *Chemical Engineering and Technology*, vol. 21, No. 4, pp. 297-303, 1999.

[10]   J. Miwa, Y. Asako, C. Hong, and M. Faghri, "Performance of gas-to-gas micro-heat exchangers", *Journal of Heat Transfer*, vol. 131, No. 5, pp. 051801-1-051801-9, May 2009.

[11]   K. Koyama, and Y. Asako, "Experimental investigation on heat transfer characteristics of a gas-to-gas counterflow microchannel heat exchanger", *Experimental Heat Transfer*, 2009, In press.

[12]   R. K. Shah, and A. L. London, *Laminar Flow Forced Convection in Ducts, Advances in Heat Transfer Supplement 1*, Academic Press: New York, 1978.

[13]   W. M. Kays, and A. L. London, *Compact Heat Exchangers, A Summary of Basic Heat Transfer and Flow Friction Design Data*, McGraw-Hill: New York, 1958.

[14]   J. M. Yin, C. W. Bullard, and P. S. Hrnjak, "Single-phase pressure drop measurements in a microchannel heat exchanger", *Heat Transfer Engineering*, vol. 23, No. 4, July 2002.